

Electron cooling by diffusive normal metal–superconductor tunnel junctionsA. S. Vasenko,¹ E. V. Bezuglyi,² H. Courtois,³ and F. W. J. Hekking¹¹*LPMMC, Université Joseph Fourier and CNRS, 25 Avenue des Martyrs, BP 166, 38042 Grenoble, France*²*Institute for Low Temperature Physics and Engineering, Kharkov 61103, Ukraine*³*Institut Néel, CNRS and Université Joseph Fourier, 25 Avenue des Martyrs, BP 166, 38042 Grenoble, France*

(Received 22 December 2009; published 15 March 2010)

We investigate heat and charge transport in NN'IS tunnel junctions in the diffusive limit. Here, N and S are massive normal and superconducting electrodes (reservoirs), N' is a normal metal strip, and I is an insulator. The flow of electric current in such structures at subgap bias is accompanied by heat transfer from the normal metal into the superconductor, which enables refrigeration of electrons in the normal metal. We show that the two-particle current due to Andreev reflection generates Joule heating, which is deposited in the N electrode and dominates over the single-particle cooling at low enough temperatures. This results in the existence of a limiting temperature for refrigeration. We consider different geometries of the contact, one dimensional and planar, which are commonly used in the experiments. We also discuss the applicability of our results to a double-barrier SINIS microcooler.

DOI: [10.1103/PhysRevB.81.094513](https://doi.org/10.1103/PhysRevB.81.094513)

PACS number(s): 74.45.+c, 74.50.+r, 74.40.Gh, 74.25.fc

I. INTRODUCTION

The flow of electric current in normal metal–insulator–superconductor (NIS) tunnel junctions is accompanied by heat transfer from the normal metal into the superconductor.^{1–3} This phenomenon arises due to selective tunneling of high-energy quasiparticles out of the normal metal which is induced by the superconducting energy gap. It is similar to the Peltier effect in metal–semiconductor contacts⁴ and enables refrigeration of electrons in the normal metal. The heat current out of the normal metal (also referred to as “cooling power”) is maximal at a voltage bias just below the energy gap, $eV \lesssim \Delta$. For $eV \gtrsim \Delta$, both the current I through the junction and the Joule heating power IV strongly increase, rendering the cooling power negative.

A micrometer-sized refrigerator, based on a NIS tunnel junction, has been first fabricated by Nahum *et al.*¹ The authors used a single NIS junction in order to cool a small normal metal strip. Later, Leivo *et al.*⁵ noticed that the cooling power is an even function of the applied voltage and fabricated a refrigerator with two NIS junctions arranged in a symmetric series configuration (SINIS). This results in reduction of the electron temperature from 300 to about 100 mK, offering perspectives for the use of NIS junctions for on-chip cooling of nanosized systems, such as high-sensitive detectors and quantum devices.⁶ To enhance the performance of NIS microcoolers, it is important to understand possible limitations of the NIS refrigeration.

Serious limitations of the cooling effect arise from the fact that nonequilibrium quasiparticles injected into the superconducting electrode accumulate near the tunnel interface.^{7,8} The consequences are the backtunneling of hot quasiparticles to the normal metal,^{8,9} the emission of phonons (by the recombination of nonequilibrium quasiparticles into Cooper pairs) that partially penetrate the normal metal,^{7,9} and the overheating of the superconducting electrode.⁷ All these effects reduce the efficiency of NIS refrigerators. This problem can be solved by imposing a local thermal equilibrium in the superconducting electrode.⁸ So-called quasiparticle traps,^{10,11}

made of an additional normal metal layer covering the superconducting electrode, remove hot quasiparticles from the superconductor and are thus beneficial in this respect.

However, there is a fundamental limitation for NIS microcoolers. It arises from the intrinsic multiparticle nature of current transport in NIS junctions which is governed not only by single-particle tunneling but also by two-particle (Andreev) tunneling. The single-particle current and the associated heat current are due to quasiparticles with energies $E > \Delta$ (compared to the Fermi level). At very low temperatures, single-particle processes are exponentially suppressed in the subgap voltage region $eV < \Delta$ and the charge is mainly transferred by means of Andreev reflection of quasiparticles with energies $E < \Delta$.^{12,13} The Andreev current I_A does not transfer heat through the NS interface but rather generates the Joule heating $I_A V$ which is deposited in the normal metal electrode¹⁴ and dominates single-particle cooling at low-enough temperatures. Thus the interplay between the single-particle tunneling and Andreev reflection sets a limiting temperature for the refrigeration.

The role of the Andreev current in the electron refrigeration has been first theoretically analyzed by Bardas and Averin for the simplest model of the NIS microcooler—a one-dimensional (1D) constriction between the N and S reservoirs,¹⁵ assuming the constriction length to be much shorter than the coherence length. In experiment, the importance of Andreev processes in NIS microcoolers was first demonstrated by Rajauria *et al.*¹⁴ by using the theoretical estimations of the Andreev current,¹⁶ obtained within the tunnel Hamiltonian technique, for interpretation of the experimental data. In this paper, we present a quantitative analysis of heat transport in diffusive NIS tunnel junctions based on the solution of microscopic equations of nonequilibrium superconductivity.¹⁷ We consider the general case of arbitrary length of the normal wire, as well as of different possible geometries of the junction: one-dimensional junctions and planar junctions with overlapping thin-film electrodes, commonly used in experiments.¹⁴ We also discuss the applicability of our results to a double-barrier SINIS microcooler.

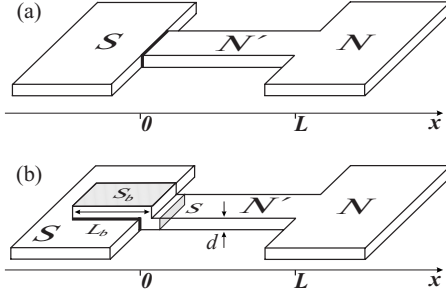


FIG. 1. (a) One-dimensional and (b) planar models of the NN'IS junction. The insulating barrier is shown by thick black line.

The paper is organized as follows. In the next section, we develop a theory for 1D junctions. We start with a discussion of basic equations and adopted approximations, calculate the spectral characteristics of the junction using Usadel equations, and finally obtain both the electric and the heat currents through the junction. In Sec. III, we extend this theory to the case of planar junctions. We discuss the results in Sec. IV and then consider possible extension of our theory to the case of a double-barrier SINIS junction in Sec. V. Finally, we summarize the results in Sec. VI.

II. 1D NN'IS JUNCTION MODEL

A. Basic equations

The model of the one-dimensional NN'IS junction is depicted in Fig. 1(a). It consists of a voltage-biased normal metal reservoir (N) and a normal metal wire (N') of length L connected to a superconducting reservoir (S) through an insulator layer (I). We assume the NN' interface to be fully transparent.

In our theoretical analysis, we consider the diffusive limit, in which the superconducting coherence length is given by expression $\xi_0 = \sqrt{D/2\Delta}$, where D is the diffusion coefficient of the normal metal (we assume $\hbar = k_B = 1$) and the elastic scattering length $\ell \ll \xi_0$. In this case, calculation of the electric and heat currents requires solution of the one-dimensional Keldysh-Usadel equations¹⁷ (see also the review¹⁸) for the 4×4 matrix Keldysh-Green function $\check{G}(x, E)$ in the N' lead,

$$[\sigma_z E, \check{G}] = iD \partial_x \check{J}, \quad \check{J} = \check{G} \partial_x \check{G}, \quad \check{G}^2 = 1, \quad (1)$$

$$\check{G} = \begin{pmatrix} \hat{g}^R & \hat{G}^K \\ 0 & \hat{g}^A \end{pmatrix}, \quad \hat{G}^K = \hat{g}^R \hat{f} - \hat{f} \hat{g}^A. \quad (2)$$

Here, σ_z is the Pauli matrix, $\partial_x \equiv \partial / \partial x$, $\hat{g}^{R,A}$ are the 2×2 Nambu matrix retarded and advanced Green functions, and $\hat{f} = f_+ + \sigma_z f_-$ is the matrix distribution function (we use ‘‘check’’ for 4×4 and ‘‘hat’’ for 2×2 matrices). In Eq. (1) we neglect the inelastic collision term, assuming the length L of the N' lead to be smaller than the inelastic relaxation length.

Equation (1) can be decomposed into the diffusion equations for the Green's functions

$$[\sigma_z E, \hat{g}] = iD \partial_x \hat{J}, \quad \hat{J} = \hat{g} \partial_x \hat{g}, \quad \hat{g}^2 = 1 \quad (3)$$

and the equation for the Keldysh component \hat{G}^K ,

$$[\sigma_z E, \hat{G}^K] = iD \partial_x \hat{J}^K, \quad \hat{J}^K = \hat{g}^R \partial_x \hat{G}^K + \hat{G}^K \partial_x \hat{g}^A. \quad (4)$$

Taking into account the normalization condition $\hat{g}^2 = 1$, we parameterize the Green's function by the complex spectral angle θ ,

$$\hat{g}(x, E) = \sigma_z \cosh \theta + i \sigma_y \sinh \theta. \quad (5)$$

The electric and energy currents are related to the Keldysh component of the matrix current \check{J} as¹⁷⁻²⁰

$$I = \frac{g_N}{e} \int_0^\infty I_- dE, \quad Q = \frac{g_N}{e^2} \int_0^\infty EI_+ dE, \quad (6)$$

$$I_- \equiv \frac{1}{4} \text{Tr} \sigma_z \hat{J}^K = D_- \partial_x f_-, \quad I_+ \equiv \frac{1}{4} \text{Tr} \hat{J}^K = D_+ \partial_x f_+, \quad (7)$$

where g_N is the normal conductance of the N' lead per unit length and D_\pm are dimensionless diffusion coefficients,

$$D_- = (1/4) \text{Tr} (1 - \sigma_z \hat{g}^R \sigma_z \hat{g}^A) = \cosh^2(\text{Re } \theta), \quad (8a)$$

$$D_+ = (1/4) \text{Tr} (1 - \hat{g}^R \hat{g}^A) = \cos^2(\text{Im } \theta). \quad (8b)$$

Here we expressed the advanced Green's functions through the retarded ones using the general relation $\hat{g}^A = -\sigma_z \hat{g}^{R\dagger} \sigma_z$,¹⁷ then omitted the superscript R . The quantity I_+ has the meaning of the spectral density of the net probability current of electrons and holes, while I_- represents the spectral density of the electron-hole imbalance current responsible for the charge transfer (see the discussion in Refs. 18 and 21). Calculation of the electric and energy currents in Eqs. (6) involves two steps: first one has to solve the diffusion Eqs. (3) for the spectral angle θ and then to solve the kinetic Eqs. (4) to find the distribution functions.

The expression for the heat current out of the normal metal reservoir (cooling power) in a diffusive NIS structure was suggested by Bardas and Averin in Ref. 15. In contrast to the ballistic case (also discussed in Ref. 15), its spectral density contains several additional terms which are odd in energy and therefore vanish upon integration over energy. We propose another method for the derivation of the cooling power, which seems to be physically clearer and does not involve the nonphysical, odd-in-energy terms. We define the heat generation in the reservoir through the work done by the applied voltage on the nonequilibrium quasiparticles coming to this reservoir, i.e., through the change of the kinetic energy E_k of the quasiparticles. We accept the definition $E_k^e = E - e\varphi(x)$ for the electronlike and $E_k^h = E + e\varphi(x)$ for the holelike quasiparticles, where $\varphi(x)$ is the electric potential (note that the quantity E is the total quasiparticle energy which is conserved during passage across the junction, in contrast to E_k). Along this line of reasoning, the heat generation in a given reservoir can be defined as the kinetic energy flow to that reservoir

$$I_k(x) = \pm N_F S \int_{-\infty}^{\infty} [E_k^e(x) I^e + E_k^h(x) I^h] dE. \quad (9)$$

We take $x=0$ and the minus sign for the left S reservoir and $x=L$ and the plus sign for the right N reservoir; N_F is the electron density of states per spin in the normal state, S is the cross-sectional area of the junction, and the quantities I^e and I^h are the electron and hole probability flow densities, respectively. The expressions for I^e and I^h were found in Ref. 21 by introducing the following parametrization of the matrix distribution function (see also Ref. 18),

$$\hat{f} = 1 - 2 \begin{pmatrix} n^e & 0 \\ 0 & n^h \end{pmatrix}, \quad n^{e,h} = \frac{1}{2}(1 - f^{e,h}), \quad f^{e,h} = f_{\pm} \pm f_{\mp}.$$

The functions n^e and n^h have the meaning of the electron and hole population numbers, respectively, and approach the Fermi distribution in the reservoirs. Then the electron and hole probability currents are defined as²¹

$$I^{e,h} = (1/2) \mathcal{D}(I_{\pm} \pm I_{\mp}) \\ = - (1/2) \mathcal{D}[(D_{\pm} \pm D_{\mp}) \partial_x n^e + (D_{\pm} \mp D_{\mp}) \partial_x n^h]. \quad (10)$$

In the N reservoir ($\theta=0$, $D_{\pm}=1$), the currents $I^{e,h}$ are naturally related to the electron and hole diffusion flows, $I^{e,h} = -\mathcal{D} \partial_x n^{e,h}$. Within the N' lead, each current $I^{e,h}$ generally consists of a combination of both electron and hole diffusion flows, which reflects the coherent mixing of electron and hole states in the proximity region. Upon substitution of Eq. (10) into Eq. (9), using the relation $g_N = 2e^2 N_F \mathcal{D} S$, we obtain the well-known equation for the heat current out of the normal metal reservoir (cooling power)

$$P = -I_k(L) = -IV - Q. \quad (11)$$

In the case of a NIN (normal metal-insulator-normal metal) structure, the heat generation in both reservoirs was found to be equal to $IV/2$.²² For the NIS structure, it is the imbalance between the kinetic energy flows to the N and S reservoirs that leads to the cooling effect. The heat P taken from the N electrode is then released in the S reservoir, $I_k(0) = -Q = P + IV$, thus the full heat production in both reservoirs is equal to the Joule heating, $I_k(0) + I_k(L) = IV$.

Now we discuss the boundary conditions. At $x=L$, we assume all functions to be continuous, neglecting a spreading resistance of the transparent NN' interface: in the diffusive limit, this resistance is always small compared to the resistance of the N' wire.²³ At the tunnel barrier, $x=0$, the function \check{G} and the matrix current \check{J} at the normal (N') and the superconducting (S) sides of the junction are connected via the generalized boundary condition due to Nazarov²⁴

$$\check{J}_{N'} = \frac{1}{2g_N R_T} \int_0^1 \frac{\Gamma \rho(\Gamma) d\Gamma [\check{G}_S, \check{G}_{N'}]}{1 + \frac{\Gamma}{4} (\{\check{G}_S, \check{G}_{N'}\} - 2)}, \quad (12)$$

where R_T is the barrier resistance and $\rho(\Gamma)$ is the distribution of the transparencies of the conducting channels of the barrier [$\int_0^1 \Gamma \rho(\Gamma) d\Gamma = 1$]. Assuming the absence of highly transparent channels with $\Gamma \sim 1$ and considering $\rho(\Gamma)$ to be local-

ized around a small value of $\Gamma \ll 1$ (tunnel limit), we can neglect the anticommutator term in Eq. (12), thus arriving at the Kupriyanov-Lukichev boundary condition²⁵ at $x=0$,

$$\check{J}_{N'} = (2g_N R_T)^{-1} [\check{G}_S, \check{G}_{N'}]. \quad (13)$$

The boundary conditions for the functions \hat{g} and \hat{G}^K at the tunnel barrier follow from Eq. (13),

$$\hat{J}_{N'} = (W/\xi_0) [\hat{g}_S, \hat{g}_{N'}], \quad (14a)$$

$$\hat{J}_{N'}^K = (W/\xi_0) [\check{G}_S, \check{G}_{N'}]^K. \quad (14b)$$

Here, the tunneling parameter W is defined as

$$W = R(\xi_0)/2R_T = (3\xi_0/4\ell)\Gamma \gg \Gamma, \quad (15)$$

where $R(\xi_0) = \xi_0 g_N^{-1}$ is the resistance of the N' lead per length ξ_0 . It has been shown in Refs. 26 and 27 that it is this quantity, rather than the barrier transparency Γ , that plays the role of the transparency parameter for diffusive tunnel junctions. Below we consider the case $W \ll 1$, which corresponds to the conventional tunneling limit.

The N and S electrodes are assumed to be equilibrium reservoirs with unperturbed spectral characteristics and equilibrium quasiparticle distributions

$$\theta_N = 0, \quad f_{\pm N} = \frac{1}{2} \left(\tanh \frac{E + eV}{2T_N} \pm \tanh \frac{E - eV}{2T_N} \right), \quad (16)$$

$$\theta_S = \text{arctanh} \frac{\Delta}{E}, \quad f_{+S} = \tanh \frac{E}{2T_S}, \quad f_{-S} = 0, \quad (17)$$

where T_N and T_S are the temperatures of the N and S reservoirs, respectively.

Using the parametrization in Eq. (5), we rewrite Eq. (3) as the Usadel equation²⁸ for the spectral angle $\theta(E, x)$,

$$i\mathcal{D} \partial_x^2 \theta = 2E \sinh \theta. \quad (18)$$

Here and below, we omit the subscript N' for the functions f_{\pm} and θ in the N' lead. The boundary conditions for Eq. (18) follow from Eqs. (16) and (14a),

$$\theta|_{x=L} = 0, \quad (19a)$$

$$\partial_x \theta|_{x=0} = (2W/\xi_0) \sinh(\theta_0 - \theta_S), \quad (19b)$$

where θ_0 denotes the value of θ at $x=0$.

The kinetic equations for the functions f_{\pm} follow from Eq. (4) and have the form of conservation laws for the spectral currents I_{\pm} ,

$$D_{\pm} \partial_x f_{\pm} = I_{\pm} = \text{const}. \quad (20)$$

The continuity of the distribution functions at the N'N interface implies the conditions $f_{\pm}(E, L) = f_{\pm N}(E)$. The boundary conditions at the SN' interface follow from Eq. (14b),²¹

$$g_N I_{-}(E) = G_T^{-}(E) f_{-0}(E), \quad (21a)$$

$$g_N I_{+}(E) = G_T^{+}(E) [f_{+0}(E) - f_{+S}(E)], \quad (21b)$$

where the subscript 0 denotes the function values at $x=0$ and

$$G_T^\pm(E) = R_T^{-1}(N_S N_{N'} \mp M_S^\pm M_{N'}^\pm), \quad (22)$$

$$N(E) = \text{Re}(\cosh \theta), \quad M^+(E) + iM^-(E) = \sinh \theta.$$

The function $N(E)$ is the density of states (DOS) normalized to its value N_F in the normal state; the quantities G_\pm can be interpreted as spectral conductances of the tunnel barrier for the probability (+) and electric (−) currents, respectively. At large energies, $|E| \gg \Delta$, when $N(E)$ approaches unity and the condensate spectral functions $M^\pm(E)$ turn to zero at both sides of the interface, the conductances $G_T^\pm(E)$ coincide with the normal barrier conductance, R_T^{-1} . Within the subgap region $|E| < \Delta$, $G_T^\pm(E)$ turn to zero, which reflects blocking of the probability current due to full Andreev reflection.

In the superconducting reservoir, the density of states $N_S(E)$ and the condensate spectral functions $M_S^\pm(E)$ read

$$N_S(E) = \frac{|E|\Theta(|E| - \Delta)}{\sqrt{E^2 - \Delta^2}}, \quad (23a)$$

$$M_S^-(E) = -\frac{\Delta\Theta(\Delta - |E|)}{\sqrt{\Delta^2 - E^2}}, \quad M_S^+(E) = \frac{\Delta\Theta(|E| - \Delta)}{\sqrt{E^2 - \Delta^2}}, \quad (23b)$$

where $\Theta(x)$ is the Heaviside step function.

B. Solution of the Usadel and kinetic equations

Generally, the solution of the Usadel equation for a N' lead of finite length can be found only numerically. However, in the case of a low-transparent tunnel barrier, $W \ll 1$, the spectral angle is small, $\theta \ll 1$, for all essential energies, which enables us to linearize Eqs. (18) and (19b),

$$iD\partial_x^2\theta = 2E\theta, \quad (24a)$$

$$\partial_x\theta|_{x=0} = (2W/\xi_0)(\theta_0 \cosh \theta_S - \sinh \theta_S). \quad (24b)$$

The analytical solution of these linearized equations,

$$\theta(E, x) = \theta_0(E) \frac{\sinh[k_N(L - x)/\xi_0]}{\sinh[k_N L/\xi_0]}, \quad k_N = \sqrt{\frac{E}{i\Delta}}, \quad (25)$$

$$\theta_0(E) = \frac{2W \sinh \theta_S}{k_N \coth(k_N L/\xi_0) + 2W \cosh \theta_S}, \quad (26)$$

was found to differ from the numerical solution of the exact, nonlinearized Usadel equation by less than 1% for reasonable values of $W \leq 10^{-2}$. Note that in our approximation, we keep a small term of the order of W in the denominator of Eq. (26) which prevents divergence of θ_0 at the gap edge, $E = \Delta$, and thus provides a good agreement with the numerical solution in the vicinity of this “dangerous” point.

The analytic solution of the kinetic Eq. (20) with corresponding boundary conditions (20) is

$$f_- = f_{-N} - \frac{f_{-N} R_N \alpha_-(x)}{R_T^-(E) + R_N \alpha_-(0)}, \quad (27a)$$

$$f_+ = f_{+N} - \frac{(f_{+N} - f_{+S}) R_N \alpha_+(x)}{R_T^+(E) + R_N \alpha_+(0)}, \quad (27b)$$

$$\alpha_\pm(x) = \int_x^L \frac{dx'}{L} D_\pm^{-1}(E, x'),$$

where $R_T^\pm(E) = [G_T^\pm(E)]^{-1}$ are spectral resistances of the tunnel barrier²¹ and $R_N = Lg_N^{-1}$ is the normal resistance of the N' lead. In Eqs. (27), we used the relation

$$R_{N'}/R_T = 2W(L/\xi_0), \quad (28)$$

following from the definition of the parameter W in Eq. (15). In a typical experimental situation, the tunnel resistance dominates, $R_T \gg R_N$, therefore the functions f_\pm are always close to the equilibrium distributions $f_{\pm N}$ in the N reservoir.

C. Electric current

The electric current is given by the equation obtained by combining Eqs. (6), (21a), and (27a),

$$I = \frac{1}{e} \int_0^\infty \frac{f_{-N}(E)}{R_T^-(E) + R_{N'}^-(E)} dE, \quad R_{N'}^-(E) = R_N \alpha_-(0). \quad (29)$$

A similar result has been obtained for a NINIS structure in Refs. 21 and 29; it differs from Eq. (29) by an additional tunnel resistance of the NIN interface in the denominator. In the spirit of circuit theories for mesoscopic superconducting structures,^{21,24} this equation can be interpreted as “Ohm’s law” for the spectral current induced by the effective potential f_{-N} in the series of the tunnel resistance R_T^- and the resistance $R_{N'}^-$ of the N' lead renormalized by the proximity effect.

The current in Eq. (29) involves contributions of both the single-particle and the two-particle (Andreev) currents. It is useful to discuss these two components separately. To this end, we divide the total range of energy integration into two regions, $E > \Delta$ and $0 < E < \Delta$, and take into account that the superconducting DOS $N_S(E) = 0$ at $0 < E < \Delta$ and the spectral function $M_S^-(E) = 0$ at $E > \Delta$,

$$I = I_1 + I_A = \frac{1}{e} \int_\Delta^\infty \frac{f_{-N}(E)}{R_T^-(N_S N_{N'})^{-1} + R_{N'}^-(E)} dE + \frac{1}{e} \int_0^\Delta \frac{f_{-N}(E)}{R_T^-(M_S^- M_{N'}^-)^{-1} + R_{N'}^-(E)} dE. \quad (30)$$

The main contribution to the current I_1 comes from the processes of single-particle tunneling. Besides, I_1 contains small proximity corrections due to deviations of the DOS $N_{N'}$ and of the diffusion coefficient D_- in the N' lead from their unperturbed values $N_{N'} = D_{N'} = 1$. Physically, these deviations are due to the partial Andreev reflection at the energies above the superconducting gap and therefore rapidly decay as the energy increases. Neglecting this small effect, we obtain the formula

$$I_1 = \frac{1}{e} \int_{\Delta}^{\infty} \frac{f_{-N}(E)}{R_T N_S^{-1} + R_N} dE, \quad (31)$$

which describes the single-particle current in the NN'IS structure. At the subgap voltages, $eV < \Delta$, this current tends to zero exponentially at small temperatures, $T_N \ll \Delta$. At large voltage, $eV \gg \Delta$, the current I_1 approaches an Ohmic dependence with the deficit current arising from the contribution of the N' lead to the net junction resistance $R = R_T + R_N$,

$$I_1 \approx \frac{V}{R} - I_{def}, \quad I_{def} \approx \frac{r\Delta}{eR} \ln \frac{\sqrt{2}}{r}, \quad r = \frac{R_N}{R_T}. \quad (32)$$

Finally, neglecting the small contribution R_N to the junction resistance and rewriting f_{-N} in terms of the Fermi function of the N reservoir, $n_N(E) = [1 + \exp(E/T_N)]^{-1}$, we arrive at the standard formula of the tunnel theory,³⁰

$$I_1 = \frac{1}{eR_T} \int_{-\infty}^{\infty} N_S(E) [n_N(E - eV) - n_N(E)] dE. \quad (33)$$

Within the same approximations, the Andreev current is reduced to the following form:

$$I_A = \frac{2W\Delta^2}{eR_T} \int_0^{\Delta} \frac{g_+}{g_+^2 + (g_- + 2WE)^2} \frac{f_{-N}(E)}{\sqrt{\Delta^2 - E^2}} dE. \quad (34)$$

$$g_{\pm}(E) = \frac{\sinh \beta \pm \sin \beta}{\cosh \beta - \cos \beta} \sqrt{\frac{E(\Delta^2 - E^2)}{2\Delta}}, \quad \beta = \sqrt{\frac{2E}{\Delta}} \frac{L}{\xi_0}.$$

At large voltage, $eV \gg \Delta$, the Andreev current approaches a constant value $I_{exc} \approx (\sqrt{2}W\Delta/eR)\ln(\sqrt{2}/W)$ (excess current); for long junctions, $L \gg \xi_0$, it is much smaller than the single-particle deficit current in Eq. (32). Thus in this limit, the net electric current, $I_1 + I_A$, always exhibits a deficit current. The Andreev current in NIS structures was first calculated microscopically by Hekking and Nazarov¹⁶ (see also Ref. 31) and Volkov *et al.*³² Note that in our consideration, we neglect possible pair-breaking factors (such as magnetic impurities) and damping of quasiparticles in the S region due to inelastic interactions. For this reason, our results concerning Andreev current may differ from that by Volkov *et al.*,^{32,33} especially at small eV comparable with corresponding relaxation rates.

We would like to notice that the Andreev current does not depend on the N' lead length L as long as $L \gg \xi_0$. In this case, the magnitude of the Andreev current at $eV \sim \Delta$ can be estimated from Eq. (34) as $I_A \sim W\Delta/eR_T = \Delta R(\xi_0)/2eR_T^2$. This reproduces the result of Hekking and Nazarov¹⁶ and Volkov *et al.*³² As energy decreases, the spectral density of the Andreev current [the integrand in Eq. (34)] diverges as $E^{-1/2}$ until E reaches the small Thouless energy $E_{Th} = D/L^2$, which plays the role of a cutoff factor. Such behavior of the Andreev current was first discovered in Ref. 16 using the diagrammatic methods in the tunnel Hamiltonian formalism. In the limit of a short junction, $L \ll \xi_0$, when the proximity effect and the Andreev current are suppressed by the N reservoir, we recover the result of Bardas and Averin,¹⁵ $I_A \sim \Delta R(L)/2eR_T^2 = \Delta R_N/2eR_T^2$.

D. Energy current

The energy current can be obtained upon combining Eqs. (6), (21b), and (27b),

$$Q = \frac{1}{e^2} \int_0^{\infty} E \frac{f_{+N}(E) - f_{+S}(E)}{R_T^+(E) + R_N^+(E)} dE, \quad R_N^+(E) = R_N \alpha_+(0). \quad (35)$$

This expression is quite similar to Eq. (29) for the electric current and has the same physical interpretation: the spectral probability current flowing through the series of the tunnel and normal resistances is determined by Ohm's law for the effective potential difference $f_{+N} - f_{+S}$.

First, we note that the energy integration in Eq. (35) is actually confined to the interval $E > \Delta$ since the conductivity G_T^+ turns to zero (and, correspondingly, $R_T^+ \rightarrow \infty$) at $0 < E < \Delta$. Thus the Andreev energy current Q_A is identically zero; physically, this corresponds to the fact that the quasi-particle probability current I_+ is completely blocked in the subgap energy region due to full Andreev reflection.

Neglecting the proximity corrections to the spectral functions, i.e., assuming $N_{N'} = D_+ = 1$ and $M_{N'}^+ = 0$, we obtain a simplified form of the single-particle energy current

$$Q_1 = \frac{1}{e^2} \int_{\Delta}^{\infty} E \frac{f_{+N}(E) - f_{+S}(E)}{R_T N_S^{-1} + R_N} dE. \quad (36)$$

Finally, omitting the contribution R_N of the normal lead to the total resistance and expressing f_+ in terms of the Fermi functions, we arrive at the standard form for the energy current

$$Q_1 = - \frac{1}{e^2 R_T} \int_{-\infty}^{+\infty} N_S(E) E [n_N(E - eV) - n_S(E)] dE, \quad (37)$$

where $n_S(E) = [1 + \exp(E/T_S)]^{-1}$ is the Fermi function of the S reservoir.

E. Heat current

The heat current out of the normal metal reservoir (cooling power) can now be obtained from the above expressions for the electric and the energy currents, Eqs. (30) and (35), using Eq. (11). As follows from Eq. (11), the Andreev heat current to the normal reservoir is nonzero, giving a negative contribution P_A to the cooling power

$$P = P_1 + P_A, \quad P_A = -I_A V. \quad (38)$$

From this equation, we see that the heat current out of the normal metal is affected by the Joule heating generated by the Andreev current I_A . This is due to the fact that the Andreev current is fully dissipated in the normal metal.

Using the tunnel model formula (33) for the electric current and Eq. (37) for the energy current, we arrive at the well-known form for the cooling power⁵

$$P_1 = \frac{1}{e^2 R_T} \int_{-\infty}^{+\infty} N_S(E)(E - eV)[n_{N'}(E - eV) - n_S(E)]dE. \quad (39)$$

This equation is widely used when fitting the experimental data on electron cooling. Such an approach is valid as long as the Andreev contribution to the electric current is negligibly small, i.e., at moderately high temperatures. As noted above, at low temperatures, the single-particle processes are exponentially suppressed in the subgap voltage region, where the effect of Andreev current on electron cooling becomes essential and must be taken into account.

III. PLANAR NN'IS MODEL

In this section, we present an extension of the approach developed above to the more realistic case of a sandwich-type tunnel junction with a thin-film N' lead as sketched in Fig. 1(b). This situation is more complex; however, it is possible to reduce this problem to the 1D case by formulating effective boundary conditions at the junction, following a method suggested by Volkov³³ and Kupriyanov.³⁴

In the general three-dimensional case, the Keldysh-Usadel Eq. (1) and the boundary condition Eq. (13) read

$$[\sigma_z E, \check{G}] = iD \nabla \check{J}, \quad \check{J} = \check{G} \nabla \check{G}, \quad (40a)$$

$$\mathbf{n} \check{J}_{N'} = (2g_N R_T)^{-1} [\check{G}_S, \check{G}_{N'}], \quad (40b)$$

where \mathbf{n} is a vector normal to the insulator layer. In Eq. (40b), all functions are taken at the sides of the barrier.

We suppose the size of the planar junction L_b to exceed the coherence length, $L_b \gg \xi_0$, and the thickness of the N' lead to be much smaller than the coherence length, $d \ll \xi_0$. Then the function \check{G} in the left-hand side of Eq. (40a) is approximately constant within the normal metal bank above the junction.^{33,34} Upon integration of this equation over the volume of the normal metal bank, transforming the volume integral in the right-hand side into a surface integral, and using the boundary condition Eq. (40b) at the tunnel barrier, we obtain the effective boundary condition for the 1D Keldysh-Usadel equations in the N' lead

$$S_b d [\sigma_z E, \check{G}_{N'}] = iD \{S \check{J}_0 - S_b (W/\xi_0) [\check{G}_S, \check{G}_{N'}]\}, \quad (41)$$

where all functions are taken at the sides of the barrier. In Eq. (41), S is the cross-section area of the N' lead, d is the lead thickness, S_b is the area of the junction [see Fig. 1(b)], and $\check{J}_0 = \check{G}_{N'} \partial_x \check{G}_{N'}$ is the value of the matrix current in the N' lead at the cross-section adjoining the junction (i.e., at $x=0$). A similar result has been obtained in Ref. 35 for the case of a planar SIS junction. Equation (41) can be rewritten as

$$[\sigma_z E, \check{G}_{N'}] = 2i\Delta \{(\xi_0^2/L_b) \check{J}_0 - \tilde{W} [\check{G}_S, \check{G}_{N'}]\}, \quad (42)$$

where

$$\tilde{W} = W(\xi_0/d) = (3\xi_0^2/4\ell d)\Gamma \quad (43)$$

is the effective tunneling parameter. Note that for thin-film planar junctions, this parameter is much larger than the 1D tunneling parameter W by the ratio $\xi_0/d \gg 1$.

As long as $\xi_0 \ll L_b$ and $\xi_0 \check{J}_0 \sim W$, the first term in the right-hand side of Eq. (42) can be assumed to be the smallest one and thus neglected. However, this is only true for the Green's component of Eq. (42),

$$[\sigma_z E, \hat{g}_{N'}] = 2i\Delta \tilde{W} [\hat{g}_{N'}, \hat{g}_S], \quad (44)$$

whereas for the Keldysh component the diagonal part of the left-hand side of Eq. (42) turns to zero and therefore the boundary condition for the diagonal part of \check{J}_0^K reads

$$\check{J}_0^K = (W_f/\xi_0) [\check{G}_S, \check{G}_{N'}]^K, \quad (45a)$$

$$W_f = W(L_b/d) = W(S_b/S) = \tilde{W}(L_b/\xi_0) \gg \tilde{W}. \quad (45b)$$

The enhancement of the parameter W_f with respect to W reflects decrease of the tunnel resistance R_T compared to its value in the 1D case due to increase of the junction area from S for the 1D geometry to S_b for the planar geometry (provided the barrier transparency is equal for both cases).

In terms of the spectral angle θ in the N' lead, the boundary condition (44) has the form $k_N^2 \sinh \theta_0 = 2\tilde{W} \sinh(\theta_S - \theta_0)$ and can be solved explicitly for the boundary value θ_0 ,

$$\theta_0 = \operatorname{arctanh} \frac{2\tilde{W} \sinh \theta_S}{k_N^2 + 2\tilde{W} \cosh \theta_S}. \quad (46)$$

Equation (46) results in a DOS minigap in the normal bank of the junction. To first order in \tilde{W} , this minigap is equal to

$$\Delta_g \approx 2\tilde{W}\Delta \ll \Delta \quad (47)$$

and the spectral angle θ_0 is given by the BCS-like formula $\theta_0 \approx \operatorname{arctanh}(\Delta_g/E)$ at small energies, $E \sim \Delta_g$. The spatial dependence of the spectral angle in the N' lead obeys Eq. (25) with θ_0 defined in Eq. (46).

We note that a similar result was found for short SINIS junctions.^{36–38} The analogy between the NIS sandwich and a short SINIS junction can be clearly seen from the mapping method, similar to the one used in electrostatic problems. Indeed, at the top surface of the N bank, the boundary condition reads $\partial\theta/\partial\mathbf{n}=0$. To ensure this condition, we add a mirror image of the NIS sandwich to the top surface of the N layer, thus arriving to the problem of a SINIS junction with a normal metal interlayer of thickness $2d$.

The boundary condition (45a) for the distribution functions is similar to Eq. (14b) in the 1D case, with the substitution $W \rightarrow W_f$. As follows from the definition of the parameter W_f in Eq. (45b), the ratio of the normal and tunnel resistances is similar to Eq. (28), $R_N/R_T = 2W_f L/\xi_0$; therefore, the distribution functions in the planar geometry, being expressed in terms of the spectral resistances, coincide with the result for the 1D case, Eqs. (27). As a result, Eqs. (30)

and (35) for the electric and energy currents hold their form for the planar geometry, however, with different tunnel resistances R_T^\pm .

We note that within the main approximation in \tilde{W} , the spectral density of the Andreev current is nonzero only inside the minigap, $E \leq \Delta_g$. In this energy region, the spectral functions M_S^- and $M_{N'}^-$ are approximately equal to -1 and $-\Delta_g/(\Delta_g^2 - E^2)^{1/2}$, respectively. Using Eq. (30) and neglecting small contribution of the N' lead to the net resistance, we obtain a simple expression for the Andreev current at $eV \gg \Delta_g$ in the planar NIS junction

$$I_A = \frac{1}{eR_T} \tanh \frac{eV}{2T_N} \int_0^{\Delta_g} M_S^- M_{N'}^- dE = \frac{\pi \Delta_g}{2eR_T} \tanh \frac{eV}{2T_N}. \quad (48)$$

IV. RESULTS AND DISCUSSION

In our numerical calculations and analysis, we use exact expressions for the electric, energy, and heat currents, Eqs. (30), (35), and (11), taking into account both the proximity corrections and the resistance of the N' wire. Although these effects give small contributions to the energy and electric currents separately, the cooling power P , being a relatively small difference of the energy current and the Joule heat, is very sensitive to small details of the charge and energy transport. We will focus on the case of a planar junction which is the most adequate model of a real experimental setup. In what follows, we assume the temperatures of the N and S reservoirs to be equal, $T_N = T_S = T$.

We note that the tunneling parameters W and \tilde{W} , according to their definition in Eqs. (15) and (43), are temperature dependent, since the coherence length ξ_0 increases with temperature as $\Delta^{-1/2}(T)$. This variation is important at high-enough temperatures and it was taken into account in our calculation scheme, although at low temperatures, $T \ll T_c$, when the cooling effect becomes apparent, one may neglect the temperature dependence of Δ . In what follows, we assume the quantity W and its effective value \tilde{W} in planar junctions to be taken at $T=0$, allowing for their temperature dependence in Eq. (46) for the spectral angle by means of corresponding temperature-dependent factors. In order to keep a common scale of the cooling power P calculated for different T and \tilde{W} , we normalize P to the ratio $\Delta^2(0)/e^2 R_{T0}$, where R_{T0} is the junction resistance at a fixed value $\tilde{W}=10^{-3}$ of the tunneling parameter. Relying on typical sizes of the experimental samples, we assume $L=L_b=10\xi_0$, where the coherence length ξ_0 is taken at $T=0$ (for Al-based film structures, its value is about 100 nm).

Now we proceed to the discussion of our results. The effect of the Joule heat generated by the Andreev current I_A on the cooling power is illustrated by voltage dependencies $P(V)$ in Fig. 2, where the solid curves depict full cooling power and the dashed curves were calculated at $I_A=0$. For a highly resistive tunnel junction [$\tilde{W}=0.5 \times 10^{-3}$, Fig. 2(a)], the heating effect due to Andreev current is negligibly small. For smaller junction resistance [$\tilde{W}=2 \times 10^{-3}$, Fig. 2(b)], the

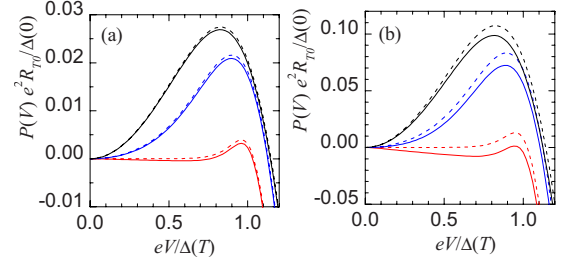


FIG. 2. (Color online) Cooling power vs bias voltage at (a) $\tilde{W}=0.5 \times 10^{-3}$ and (b) $\tilde{W}=2 \times 10^{-3}$ for different temperatures: $T=0.1T_c$ (red line), $T=0.3T_c$ (blue line), and $T=0.5T_c$ (black line). Solid lines represent full cooling power, dashed lines were computed at $I_A=0$.

heating effect essentially modifies the result; in particular, at low-enough temperature, $T=0.1T_c$, it makes $P(V)$ negative at all voltages. This is due to the fact that for phase-coherent diffusive proximity systems, the two-particle contribution to the subgap transport is anomalously strong at low energies.^{16,31}

As it is obvious from Fig. 2, the cooling power approaches a maximum at a certain optimal bias voltage V_{opt} which depends on both the temperature and the tunneling parameter. It is interesting to note that the dependence $V_{opt}(T)$ is almost universal within a wide range of the tunneling parameter, as shown in Fig. 3(a). At $T \geq 0.75T_c$, the optimal bias formally turns to zero which means that at these temperatures the cooling power becomes negative for all voltages. Existence of the upper limiting temperature for the cooling effect is explained by the increase in the number of thermally excited quasiparticles which produce enhanced Joule heat. As the temperature decreases, the optimal bias rapidly increases and approaches a value rather close to the energy gap $\Delta(T)$. Simultaneously, the cooling power at optimal bias, $P[V_{opt}(T)]$, first increases and approaches a maximum at $T \approx (0.4-0.5)T_c$ [see Fig. 3(b)]. Then, at lower temperatures, the Joule heat due to Andreev processes causes the cooling power to decrease. At a certain temperature T_{min} , the cooling power tends to zero, which defines the lower-limiting temperature for the cooling regime. As follows from Fig. 3(b), the temperature T_{min} increases with the tunnel parameter, approaching $0.24T_c$ for $\tilde{W}=10^{-2}$; this is because the Andreev current and the associated Joule heat increase with

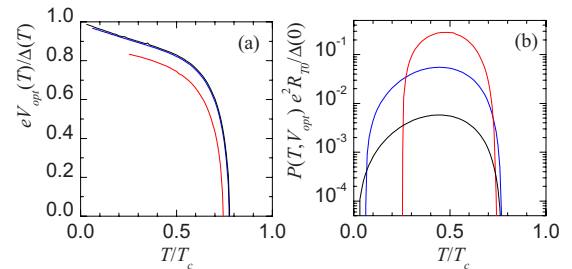


FIG. 3. (Color online) Temperature dependencies (a) of the optimum bias $V_{opt}(T)$ and (b) of the cooling power $P(T)$ at optimum bias for different values of the tunneling parameter: $\tilde{W}=10^{-4}$ (black), $\tilde{W}=10^{-3}$ (blue), and $\tilde{W}=10^{-2}$ (red).

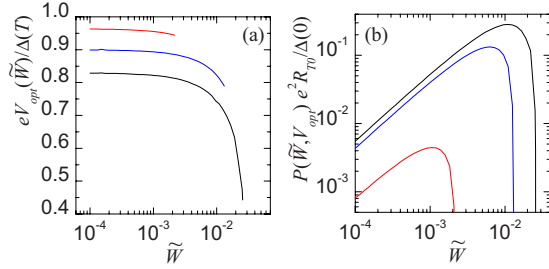


FIG. 4. (Color online) Dependencies (a) of the optimum bias $V_{opt}(\tilde{W})$ and (b) of the cooling power $P(\tilde{W})$ at optimum bias on the tunneling parameter for different temperatures: $T=0.1T_c$ (red), $T=0.3T_c$ (blue), and $T=0.5T_c$ (black).

the junction transparency more rapidly than the single-particle cooling power. At temperatures just above T_{min} , the function $P(V)$ at small applied voltage is negative, thus, the electron temperature is expected to increase first with the bias due to Andreev current heating before it decreases due to the single-particle cooling effect. This phenomenon has been observed in experiments¹⁴ at very low temperatures.

The dependencies of the optimal bias on the tunneling parameter \tilde{W} are plotted in Fig. 4(a). In accordance with the abovementioned universality of the curves $V_{opt}(T)$ for different values of \tilde{W} , the dependence $V_{opt}(\tilde{W})$ is rather weak at $\tilde{W} \leq 10^{-2}$. Within this region, the cooling power at optimal bias, $P[V_{opt}(\tilde{W})]$, linearly increases with \tilde{W} , as shown in Fig. 4(b), which is expected when single electron tunneling dominates. For larger values of the tunnel parameter, the Andreev current heating dominates over the single-particle cooling and leads to a rapid decrease of the cooling power, which tends to zero at a certain onset point, as seen from Fig. 4(b). As the temperature decreases, the role of Andreev processes becomes more important, therefore the onset shifts toward smaller values of \tilde{W} .

V. EXTENSION TO SINIS JUNCTION

As noted in Sec. I, in most experiments, the refrigerator is arranged as a double-barrier SINIS junction,¹⁴ where the S electrodes are massive reservoirs and N is a normal metal strip. Generally, in such structures, the charge and energy transport is due to multiple Andreev reflections (MAR) of quasiparticles from the NS interfaces.^{21,39} During every passage across the junction, the electrons and the retroreflected holes gain an energy eV , which allows them eventually to overcome the energy gap and to escape into the S reservoirs. This results in a strong quasiparticle nonequilibrium characterized by intense electron heating within the subgap energy region, which has been detected in the experiments.⁴⁰ From this point of view, the cooling effect observed in SINIS junction looks at a first glance somewhat surprising.

However, the inelastic scattering processes impose strong limitations for the existence of the MAR regime: in order to provide quasiparticle diffusion through the whole MAR staircase, from $-\Delta$ to Δ , the quasiparticle dwell time in the N lead, τ_d , must be smaller than the inelastic relaxation time τ_e

(for details, see Ref. 21). In typical cooling experiments on SINIS junctions with low-transparent SN interfaces,¹⁴ the dwell time greatly exceeds τ_e , which prevents accumulation of the quasiparticle energy gains and thus destroys the MAR regime. Correspondingly, the distribution functions in the N lead become close to local-equilibrium ones

$$f_{\pm}(E, x) = \frac{1}{2} \left[\tanh \frac{E + eV(x)}{2T_N} \pm \tanh \frac{E - eV(x)}{2T_N} \right], \quad (49)$$

where $V(x)$ is the voltage at the given point x . The variations in $V(x)$ are of the order of $V(R_N/R)$, i.e., negligibly small compared to the applied voltage V which mainly drops at the tunnel barriers. This implies that the distribution functions are close to equilibrium functions in a normal reservoir. In this case, the SINIS junction behaves as two NIS junctions connected in series through the equilibrium normal reservoir. As for the spectral angle, in long junctions, $L \gg \xi_0$, it can be approximated by the solution of the Usadel equation for a semi-infinite NIS structure;¹⁹ simultaneously, this solution is also a good approximation to our solution for a long NN'IS structure.

From this, we conclude that our results can be applied to the description of electron cooling in SINIS structures with large quasiparticle dwell times. Similar modeling of a SINIS junction by a series of two NIS junctions has been used in Ref. 32 for the calculation of the differential conductance.

VI. SUMMARY

We have developed a quantitative theory of charge and heat transport in one-dimensional and planar NN'IS tunnel junctions and studied the effect of electron cooling in such structures. We extend the microscopic approach by Bardas and Averin,¹⁵ originally applied to constriction-type junctions, to structures of arbitrary length and thin-film geometry used in practice for microcooler fabrication. We found that the contribution of two-particle (Andreev) current to the Joule heat generated in the normal reservoir noticeably modifies the cooling effect, especially at low temperatures and/or in rather transparent junctions. The interplay between the Andreev current heating and the single-particle cooling, whose intensity rapidly decreases with temperature, determines the lower limiting temperature T_{min} for the cooling regime. When the transparency of the NIS interface increases, the Andreev processes play a more essential role, therefore the temperature T_{min} increases. At high temperatures, the cooling regime is confined by the enhancement of the Joule heat due to thermally excited quasiparticles; the maximal cooling temperature is about $0.75T_c$, being almost independent of the junction resistance. As a result, the cooling effect persists within a specific temperature interval and approaches a maximum at the temperatures $(0.4-0.5)T_c$.

We pay special attention to the analysis of the optimum bias voltage $V_{opt}(T, \tilde{W})$, at which the cooling power approaches a maximum for given temperature T and the tunneling parameter \tilde{W} . We found that V_{opt} exhibits a virtually universal temperature dependence for different values of the tunneling parameter and approaches values close to the en-

ergy gap as long as the temperature decreases. The cooling power at optimum bias voltage first increases linearly with \tilde{W} until the Andreev current heating abruptly suppresses the cooling regime.

We discussed the applicability of our results to the description of the cooling effect in SINIS junctions. We show that such a double-barrier structure can be modeled by a series of two independent NIS junctions, provided the quasi-particle dwell time inside the junction greatly exceeds the inelastic relaxation time. This condition, which is usually satisfied in cooling experiments,¹⁴ enables one to extend the theory presented here to the case of the SINIS microcoolers.

From our considerations, we conclude that the Andreev current is one of the most serious factors of limitation of the

electron-cooling efficiency. In order to reduce this factor, one should address materials in which the proximity effect and, correspondingly, the Andreev current are strongly suppressed. A first guess to such materials can be ferromagnets.⁴¹ A quantitative analysis of the cooling effect in ferromagnet-insulator-superconductor (FIS) junctions will be presented elsewhere.

ACKNOWLEDGMENTS

The authors thank F. Giazotto, A. A. Golubov, T. T. Heikkilä, J. P. Pekola, S. Rajauria, F. Taddei, and A. F. Volkov for useful discussions. This work was supported by NanoSciERA “Nanofridge” EU project.

-
- ¹M. Nahum, T. M. Eiles, and J. M. Martinis, *Appl. Phys. Lett.* **65**, 3123 (1994).
- ²F. Giazotto, T. T. Heikkilä, A. Luukanen, A. M. Savin, and J. P. Pekola, *Rev. Mod. Phys.* **78**, 217 (2006).
- ³P. Virtanen and T. T. Heikkilä, *Appl. Phys. A: Mater. Sci. Process.* **89**, 625 (2007).
- ⁴K. Seeger, *Semiconductor Physics* (Springer, New York, 2004).
- ⁵M. M. Leivo, J. P. Pekola, and D. V. Averin, *Appl. Phys. Lett.* **68**, 1996 (1996).
- ⁶A. M. Clark, N. A. Miller, A. Williams, S. T. Ruggiero, G. C. Hilton, L. R. Vale, J. A. Beall, K. D. Irwin, and J. N. Ullom, *Appl. Phys. Lett.* **86**, 173508 (2005).
- ⁷S. Rajauria, H. Courtois, and B. Pannetier, *Phys. Rev. B* **80**, 214521 (2009).
- ⁸A. S. Vasenko and F. W. J. Hekking, *J. Low Temp. Phys.* **154**, 221 (2009).
- ⁹B. Jug and Z. Trontelj, *IEEE Trans. Appl. Supercond.* **11**, 848 (2001); *J. Phys.: Conf. Ser.* **97**, 012097 (2008).
- ¹⁰J. P. Pekola, D. V. Anghel, T. I. Suppala, J. K. Suoknuuti, A. J. Manninen, and M. Manninen, *Appl. Phys. Lett.* **76**, 2782 (2000).
- ¹¹D. Golubev and A. Vasenko, in *International Workshop on Superconducting Nano-Electronics Devices*, edited by J. Pekola, B. Ruggiero, and P. Silvestrini (Kluwer Academic, Dordrecht, 2002), p. 165.
- ¹²A. F. Andreev, *Zh. Eksp. Teor. Fiz.* **46**, 1823 (1964) [*Sov. Phys. JETP* **19**, 1228 (1964)].
- ¹³D. Saint-James, *J. Phys. (Paris)* **25**, 899 (1964).
- ¹⁴S. Rajauria, P. Gandit, T. Fournier, F. W. J. Hekking, B. Pannetier, and H. Courtois, *Phys. Rev. Lett.* **100**, 207002 (2008); *J. Low Temp. Phys.* **154**, 211 (2009).
- ¹⁵A. Bardas and D. Averin, *Phys. Rev. B* **52**, 12873 (1995).
- ¹⁶F. W. J. Hekking and Yu. V. Nazarov, *Phys. Rev. Lett.* **71**, 1625 (1993); *Phys. Rev. B* **49**, 6847 (1994).
- ¹⁷A. I. Larkin and Yu. N. Ovchinnikov, in *Nonequilibrium Superconductivity*, edited by D. N. Langenberg and A. I. Larkin (Elsevier, Amsterdam, 1986).
- ¹⁸W. Belzig, F. K. Wilhelm, C. Bruder, G. Schön, and A. D. Zaikin, *Superlattices Microstruct.* **25**, 1251 (1999).
- ¹⁹E. V. Bezuglyi and V. Vinokur, *Phys. Rev. Lett.* **91**, 137002 (2003).
- ²⁰T. Yokoyama, Y. Tanaka, A. A. Golubov, and Y. Asano, *Phys. Rev. B* **72**, 214513 (2005).
- ²¹E. V. Bezuglyi, E. N. Bratus, V. S. Shumeiko, G. Wendin, and H. Takayanagi, *Phys. Rev. B* **62**, 14439 (2000).
- ²²V. L. Gurevich, *Phys. Rev. B* **55**, 4522 (1997).
- ²³B. Nikolić and P. B. Allen, *Phys. Rev. B* **60**, 3963 (1999).
- ²⁴Yu. V. Nazarov, *Superlattices Microstruct.* **25**, 1221 (1999).
- ²⁵M. Yu. Kupriyanov and V. F. Lukichev, *Zh. Eksp. Teor. Fiz.* **94**, 139 (1988) [*Sov. Phys. JETP* **67**, 1163 (1988)].
- ²⁶M. Yu. Kupriyanov, *Pis'ma Zh. Eksp. Teor. Fiz.* **56**, 414 (1992) [*JETP Lett.* **56**, 399 (1992)].
- ²⁷E. V. Bezuglyi, E. N. Bratus', and V. P. Galaiko, *Fiz. Nizk. Temp.* **25**, 230 (1999) [*Sov. J. Low Temp. Phys.* **25**, 230 (1999)].
- ²⁸K. D. Usadel, *Phys. Rev. Lett.* **25**, 507 (1970).
- ²⁹A. F. Volkov and T. M. Klapwijk, *Phys. Lett. A* **168**, 217 (1992).
- ³⁰N. R. Werthamer, *Phys. Rev.* **147**, 255 (1966).
- ³¹H. Pothier, S. Guéron, D. Esteve, and M. H. Devoret, *Phys. Rev. Lett.* **73**, 2488 (1994).
- ³²A. F. Volkov, A. V. Zaitsev, and T. M. Klapwijk, *Physica C* **210**, 21 (1993).
- ³³A. F. Volkov, *Phys. Lett. A* **174**, 144 (1993); *Physica B* **203**, 267 (1994).
- ³⁴M. Yu. Kupriyanov, *Sov. J. Supercond.* **2**, 5 (1992).
- ³⁵E. V. Bezuglyi, A. S. Vasenko, E. N. Bratus', V. S. Shumeiko, and G. Wendin, *Phys. Rev. B* **73**, 220506(R) (2006); *Supercond. Sci. Technol.* **20**, 529 (2007).
- ³⁶R. Seviour and A. F. Volkov, *Phys. Rev. B* **61**, R9273 (2000).
- ³⁷A. Brinkman, A. A. Golubov, H. Rogalla, F. K. Wilhelm, and M. Yu. Kupriyanov, *Phys. Rev. B* **68**, 224513 (2003).
- ³⁸E. V. Bezuglyi, V. S. Shumeiko, and G. Wendin, *Phys. Rev. B* **68**, 134506 (2003).
- ³⁹M. Octavio, M. Tinkham, G. E. Blonder, and T. M. Klapwijk, *Phys. Rev. B* **27**, 6739 (1983); K. Flensberg, J. B. Hansen, and M. Octavio, *ibid.* **38**, 8707 (1988).
- ⁴⁰F. Pierre, A. Anthore, H. Pothier, C. Urbina, and D. Esteve, *Phys. Rev. Lett.* **86**, 1078 (2001).
- ⁴¹F. Giazotto, F. Taddei, R. Fazio, and F. Beltram, *Appl. Phys. Lett.* **80**, 3784 (2002).